Article

Parametric Study on the Adjustability of the Syngas Composition by Sorption-Enhanced Gasification in a Dual-Fluidized Bed Pilot Plant

Selina Hafner *, Max Schmid and Günter Scheffknecht

Institute of Combustion and Power Plant Technology (IFK), University of Stuttgart, Pfaffenwaldring 23, D-70569 Stuttgart, Germany; max.schmid@ifk.uni-stuttgart.de (M.S.); guenter.scheffknecht@ifk.uni-stuttgart.de (G.S.)
* Correspondence: selina.hafner@ifk.uni-stuttgart.de

Abstract: Finding a way for mitigating climate change is one of the main challenges of our generation. Sorption-enhanced gasification (SEG) is a process by which syngas as an important intermediate for the synthesis of e.g., dimethyl ether (DME), bio-synthetic natural gas (SNG) and Fischer–Tropsch (FT) products or hydrogen can be produced by using biomass as feedstock. It can, therefore, contribute to a replacement for fossil fuels to reduce greenhouse gas (GHG) emissions. SEG is an indirect gasification process that is operated in a dual-fluidized bed (DFB) reactor. By the use of a CO_2-active sorbent as bed material, CO_2 that is produced during gasification is directly captured. The resulting enhancement of the water–gas shift reaction enables the production of a syngas with high hydrogen content and adjustable $H_2/CO/CO_2$-ratio. Tests were conducted in a 200 kW DFB pilot-scale facility under industrially relevant conditions to analyze the influence of gasification temperature, steam to carbon (S/C) ratio and weight hourly space velocity (WHSV) on the syngas production, using wood pellets as feedstock and limestone as bed material. Results revealed a strong dependency of the syngas composition on the gasification temperature in terms of permanent gases, light hydrocarbons and tars. Also, S/C ratio and WHSV are parameters that can contribute to adjusting the syngas properties in such a way that it is optimized for a specific downstream synthesis process.

Keywords: sorption enhanced gasification; CO_2-capture; biomass; tar; synthesis
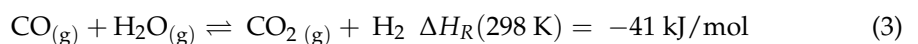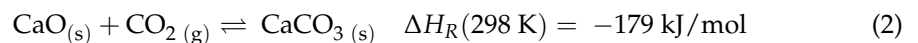
1. Introduction

On its way to becoming the first climate-neutral continent in the world, the European Union has set up the target of 40% greenhouse gas (GHG) emissions reduction compared to 1990 by 2030 with a share of renewable energy of at least 32%. In September 2020, the European commission even proposed to increase the target up to a reduction of greenhouse gases of 55% [1]. The replacement of fossil fuels in heat and power production, in the transport sector as well as in the production of chemicals by renewable energies such as biomass is one promising option that can account for meeting this target. Additionally, the reduction of greenhouse gas emissions can be supported by a more circular economy including recovering resources from waste [2,3]. One option for addressing these targets is the production of syngas out of biogenic feedstocks, residues and waste as an important intermediate [3]. Syngas can be used for the production of hydrogen and in different synthesis routes for the production of Fischer–Tropsch (FT) products, methanol (MeOH), dimethyl ether (DME), bio-synthetic natural gas (SNG) and mixed alcohols [4]. Therefore, it can contribute to a replacement of fossil fuels in different sectors (e.g., fuels for transportation, chemicals). High-quality syngases that are needed for a cost- and energy-efficient production of renewable transport fuels and chemicals are hydrogen rich, nitrogen free, have a low tar and methane content (except for bio-SNG production where a high methane content is favorable [4]) and a suitable $H_2/CO/CO_2$-ratio (e.g., module M (Equation (1)) for the respective downstream synthesis process.
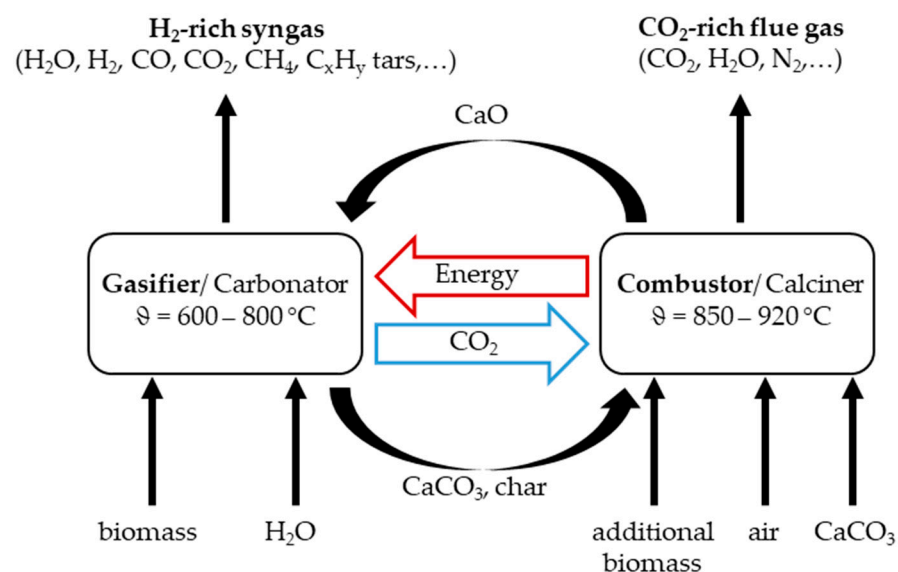
Module M

$$M = \frac{y_{H2} - y_{CO2}}{y_{CO} + y_{CO2}} \quad [-] \tag{1}$$

(y_i—gas volume fraction of component i)

Indirect steam gasification that is operated in a dual-fluidized bed (DFB) reactor has shown great potential to produce a hydrogen-rich, almost nitrogen-free and tar lean syngas without the need for pure oxygen [5,6]. This is mostly due to the use of steam as gasification agent and because of the two separate reactors. In this process, biomass is gasified with steam at temperatures between 800 and 900 °C [7,8], producing a syngas that mainly consists of hydrogen (H_2), carbon monoxide (CO), carbon dioxide (CO_2), methane (CH_4), light hydrocarbons (C_xH_y) and tars. The energy that is required for the endothermic gasification reactions is provided by the circulation of hot bed material between the gasifier and the combustor. In the combustor, unconverted char particles coming from the gasifier together with additional fuel (if necessary) are combusted with air as oxidizing agent for maintaining the required temperature for heating up the solids. Olivine was found to be a suitable bed material for indirect steam gasification as it is catalytically active towards tar reforming and has a high attrition resistance [9–11]. The process has successfully been demonstrated up to industrial scale in several facilities (e.g., Güssing, GoBiGas) [10–13]. As most of the synthesis processes require feedstock gases with higher H_2 shares than provided by indirect steam gasification, a product gas treatment is needed that comprises a water–gas shift unit followed by CO_2 removal. The sorption enhanced gasification process (SEG) (Figure 1) is a modification of the conventional indirect DFB steam gasification and uses limestone or other CO_2-active sorbents (e.g., dolomite) as bed material. In this process, CO_2 generated during gasification is directly captured by calcium oxide (CaO) forming calcium carbonate ($CaCO_3$) (carbonation, Equation (2) [14]). The removal of CO_2 from the gas phase leads to a shift in the water–gas shift (WGS) reaction (Equation (3) [15]) towards the product side, resulting in syngases with hydrogen contents of up to 75 vol% (dry basis) [16].

$$CaO_{(s)} + CO_{2\ (g)} \rightleftharpoons CaCO_{3\ (s)} \quad \Delta H_R(298\ K) = -179\ kJ/mol \tag{2}$$

$$CO_{(g)} + H_2O_{(g)} \rightleftharpoons CO_{2\ (g)} + H_2 \quad \Delta H_R(298\ K) = -41\ kJ/mol \tag{3}$$

(ΔH_R-specific reaction enthalpy)

Figure 1. Principle of the sorption-enhanced gasification (SEG) process.

As the driving force for the CO_2 capture by CaO is the difference between the partial pressure of CO_2 in the gasifier and the equilibrium partial pressure of CO_2 [8] (see $CaO/CaCO_3$ equilibrium, Figure 2), rather low gasification temperatures are required. Therefore, SEG is usually operated at gasification temperatures between 600 and 800 °C [16–18], depending on the target composition of the syngas. Despite the reduced gasification temperature compared to indirect steam gasification, the tar content in the syngas is comparatively low due to the catalytic activity of CaO towards tar reforming [8,19]. $CaCO_3$ that is formed in the gasifier is transferred into the combustor together with unconverted char particles, ash and CaO. The combustor is operated at temperatures between 900 and 920 °C at which $CaCO_3$ is regenerated to CaO and CO_2 (calcination). While the CaO is transferred back into the gasifier, CO_2 leaves the combustor with the flue gas. Due to the necessary regeneration of $CaCO_3$, the heat produced in the combustor does not only need to be sufficient for managing heat losses and endothermic gasification reactions, but also needs to provide the energy for the endothermic calcination reaction.
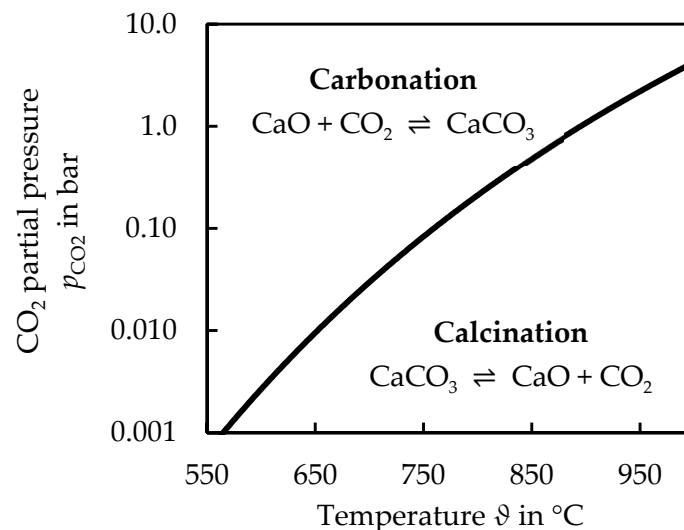

Figure 2. $CaO/CaCO_3$-equilibrium, calculation based on [20].

As a result of the in situ capture of CO_2 and the resulting enhancement of the WGS reaction in the gasifier, the module M of the syngas can be adjusted by the right choice of operational parameters (e.g., gasification temperature/bed material cycle rate, steam to carbon ratio) in such a way, that it is suitable for the respective downstream synthesis process. This enables the simplification of the gas conditioning stages after the gasifier compared to conventional gasification processes, resulting in an intensified process [17]. The SEG process can further be modified by operating the combustor in oxy-fuel mode (oxy-SEG). In this case, a part of the flue gas is recirculated and mixed with pure oxygen as oxidizing agent. As the flue gas in this process is not diluted by N_2 from the combustion air, gas streams with CO_2 concentrations >90 vol% can be achieved [21]. After purification, CO_2 can either be used in synthesis processes or permanently be stored, which gives the possibility of achieving negative CO_2 emissions making oxy-SEG to a promising CCS process [22]. According to results from Schweitzer et al. [21], changing the operation of the combustor from air to oxy-fuel combustion does not influence the composition of the syngas.

Even though CaO is catalytically active towards tar reforming, the remaining tars still need to be removed from the syngas before it can be used as feedstock in the respective synthesis process. There are different ways to remove tars from the syngas, such as washing, catalytic or thermal tar reforming and plasma-enhanced tar reforming. Independently of the tar removal process that is chosen, the tar content still is an important factor influencing

costs and efficiency of the overall process and should consequently be as low as possible in the syngas that is produced in the gasifier.

So far, the SEG process has mainly been tested for high-quality biomasses such as wood pellets/chips [7]. Drawbacks of such fuels are their relatively high costs, seasonal fluctuations, and their limited availability amongst others due to competition with other processes, which makes their use in gasification processes such as SEG challenging [21]. The usage of waste materials such as fuels based on municipal solid wastes would make the process more cost efficient and less dependent on seasonal fluctuations of the biomass availability. Due to the low gasification temperatures and the CaO containing bed material, which leads to an enhanced ash melting point [23], SEG may also be a suitable process for fuels with a low ash melting point. When using problematic feedstocks, higher tar yields and dust loads in the syngas are expected, causing additional costs for tar and particle removal. As experiments with such fuels are more complicated and more time-consuming compared to tests with high-quality biomasses, it makes sense to first establish a broad database and experiences from experiments with feedstocks that are easier to handle (e.g., wood). This allows for a better choice of appropriate operation conditions also for challenging fuels, by which time and costs can be reduced.

The aim of this study is the investigation of the main influencing parameters (gasification temperature, steam to carbon (S/C) ratio, weight hourly space velocity (WHSV)) on the syngas production via SEG with wood pellets as the reference biomass. Data were obtained in three experimental campaigns with a duration of up to 120 h each in a 200 kW DFB pilot plant located at the Institute of Combustion and Power Plant technology (IFK) at the University of Stuttgart. The facility is not electrically heated and has been operated 24/7 during the particular campaigns. The presented results lead to a better understanding of the process. The quantified influence of the investigated operation parameters and the gained operational experience will enable the successful operation of the process with more challenging fuels as well, such as municipal solid waste materials, in future.

2. Materials and Methods

2.1. Description of the Facility and Measurement Techniques

The experimental data that are presented within this work have been achieved from experiments that were conducted in the 200 kW dual-fluidized bed pilot plant that is schematically shown in Figure 3. The facility is not electrically heated, which enables conducting experiments under industrially relevant conditions. It consists of a bubbling (BFB) and a circulating fluidized bed (CFB) reactor that are both refractory lined and equipped with a water-cooling jacket. The BFB has a height of 6 m and an inner diameter of 0.33 m while the CFB has a height of 10 m with an inner diameter of 0.19 m. In the BFB (gasifier), biomass is gasified using preheated steam that enters the reactor through two gas spargers as both, fluidizing and gasifying agent. The biomass is gravimetrically dosed and fed into the reactor via a rotary valve and a screw feeder directly into the bed. Entrained solids are separated from the gas stream via primary cyclone and returned into the bed. A secondary cyclone is installed for further particle reduction before the gas is combusted in a flare and discharged through the stack. At the bottom of the reactor there is a loop seal which enables a continuous transfer of bed material into the CFB (combustor).

In the combustor, unconverted char particles coming from the gasifier are combusted with oxygen-enriched air that can be fed in three stages. Due to the relatively high heat losses in this pilot facility compared to larger-scale plants with a more favorable surface to volume ratio, additional biomass has to be fed to the combustor for enabling the required temperature that is necessary for calcination and for heating up the bed material. The addition of oxygen facilitates achieving the required heating power while maintaining the desired gas velocity. In larger-scale plants with lower load specific heat losses, the addition of oxygen would not be necessary. The use of oxygen-enriched air (y_{O2} < 50 vol.%) and the staged air supply permit the adjustment of the hydrodynamic profile in the reactor in such a way that a stable circulation of solids between both reactors and, therefore, a stable

operation of the whole process is possible. Solids that are separated from the flue gas in the primary cyclone of the combustor are split into two streams. One stream is transferred via the screw conveyor into the gasifier, while the second one is recirculated back into the combustor. The mass flow of transferred solids can be adjusted by the rotational speed of the screw and the pressure difference between both reactors. After the primary cyclone, the flue gas passes a secondary cyclone and a baghouse filter before it is released via the stack. The loop seals of both reactors are fluidized with nitrogen, which is also used for purging the pressure transducers and the rotary valves.
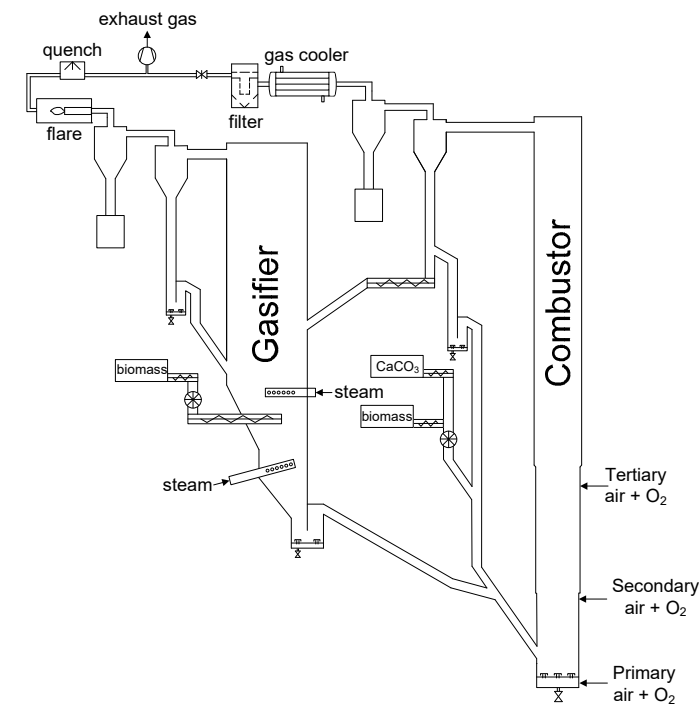
Figure 3. The 200 kW dual fluidized bed pilot scale facility at the Institute of Combustion and Power Plant technology (IFK), University of Stuttgart.

Syngas is sampled and analyzed after the cyclones using different measurement techniques. Permanent gases such as H_2, CO, CO_2, CH_4 and O_2 are analyzed continuously in a combined nondispersive infrared sensor (NDIR) and thermal conductivity analyzer (ABB AO2020 comprising Uras14 (CO, CO_2, CH_4), Magnos 106 (O_2) and Caldos 17 (H_2) components) after fine filtration, washing in isopropanol for tar removal and condensation. Lower hydrocarbons (C_xH_y) such as ethene (C_2H_4), ethane (C_2H_6), propene (C_3H_6), propane (C_3H_8) and butane (C_4H_{10}) are measured semi-continuously every 3 min after the same treatment as for the permanent gas analysis using a Varian CP-4900 Micro-GC (with a PoraPlot Q 10 m heated column) with helium as carrier gas. To evaluate the steam content, the raw syngas is analyzed after fine filtration in a Bartec Hygrophil H 4230-10 psychrometer. To analyze the tar content and composition, samples are taken wet chemically using a method developed at the Institute of Combustion and Power Plant Technology (IFK) that is described elsewhere [24] which follows the tar protocol CEN/TS 15439 [25]. Tar samples were analyzed gravimetrically using a rotary evaporator at the IFK. For evaluation of the amount of different tar components in the syngas, dedicated tar samples were sent to a laboratory at the Friedrich Alexander University in Erlangen-Nürnberg for analysis via gas chromatography and flame ionization detector (GC-FID). In the GC-FID analysis, the concentrations of the following tar components were determined: toluene, xylol, phenole, indane, indene, kresol, xylenol, napthalene, methylnaphthalene, biphenyl, acenaphthene, fluorene, phenanthrene, anthracene, fluorantene and pyrene. Below, the sum of those components is named as GC-FID tars. Tar species represented by gravimetric

and GC-FID tars are different but overlapping. While gravimetric tars represent a higher share of heavier tars, GC-FID tars represent a higher amount of lighter tars. Therefore, the values are not comparable with each other [26]. In addition to the aforementioned components, the concentration of benzene was also analyzed. The syngas volume flow is measured using a Schwing V-cone after the secondary cyclone. The flue gas volume flow is measured via a Höntzsch flow sensor and its gas composition (CO_2, CO, NO, NO_2 and SO_2) is analyzed after fine filtration and condensation with an ABB EL3020 and an EcoPhysics CLD 844 CMhr gas analyzer. Solid samples were taken frequently from both loop seals (gasifier and combustor) and analyzed in the in-house laboratory of the institute.

2.2. Experimental Procedure and Materials

Experimental results that are presented in this work were obtained in three experimental campaigns with a duration of up to 120 h each, including heat-up and shut down. The temperature trends for the gasifier and combustor during heat-up and the experimental investigations of the SEG process of one of the campaigns can be seen in Figure 4.
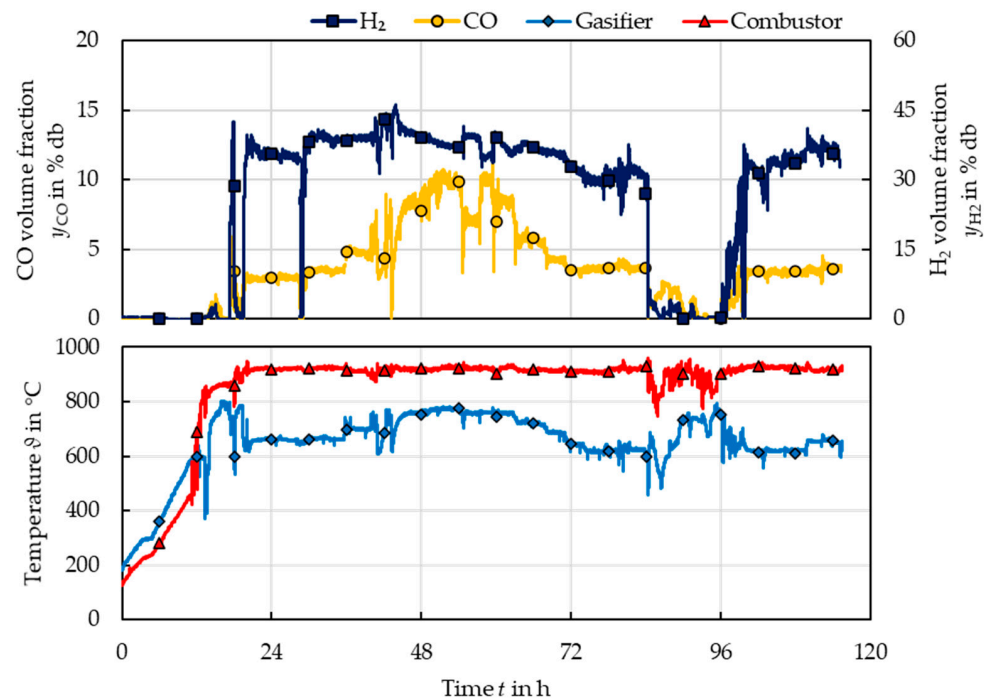
Figure 4. Trends of CO and H_2 volume fractions in the syngas and temperatures in the gasifier and combustor during an exemplary experimental campaign.

As heating up takes about 22–24 h, overnight shutdowns are not possible. Therefore, the facility is operated 24/7 in a three-shift mode. A heat-up burner that is fed with natural gas heats both reactors up until the temperatures are high enough for combustion of wood pellets, which leads to a further increase of the temperatures. While combusting wood pellets, the feeding of limestone is started to build up bed material, which is necessary for the coupling of the reactors. As soon as the reactors are heated up and the amount of bed material is sufficiently high, air that has been fed into the gasifier is replaced by superheated steam with a temperature of $145 \pm 2\,°C$ for switching to gasification.

Figure 4 shows the trends of H_2 and CO volume fractions on a dry basis under raw conditions (including purge nitrogen). Both concentrations escalate directly after the start of the gasification. Most of the changes that can be noticed afterwards are directly linked to the gasification temperature or to other modifications according to the experimental matrix, e.g., variation of the steam to carbon-ratio (S/C).

The temperature that is considered as a representative gasification temperature is measured in the middle of the gasifier bed, while the representative combustion temperature is measured at a height of 7.5 m above the gas distributor, which is upwards of the tertiary air supply. Trends for gasification and combustion temperature for an exemplary campaign can also be seen in Figure 4.

After the heat-up, the combustor temperature is kept constant above 900 °C, while the gasification temperature is being varied according to the experimental matrix by the mass flow of hot solids coming from the combustor. By enhancing the mass flow, the gasification temperature rises, but also the amount of regenerated CaO entering the reactor is increased. This can additionally affect the CO_2-capture from the syngas and should, therefore, be kept in mind when looking at the experimental results regarding the influence of the gasification temperature on the syngas composition.

For compensating bed material losses due to attrition and for enabling a good CO_2 capture, fresh limestone is continuously fed to the combustor with a ratio of fresh CaO to biomass C of 0.17 mol/mol. When calculating this ratio, additional biomass that is fed into the combustor is not considered. The limestone used has a nominal particle size of 100–300 μm and consists out of 97.5 wt% on dry basis CaO after calcination. Wood pellets of A1 quality were used as biomass. The compositions of limestone and wood pellets are shown in Tables 1 and 2 respectively.

Table 1. Limestone composition; x_i—mass fraction of component i, wf: water free, [1] Mass fraction of CO_2 that is released during calcination.

	$x_{CaO, wf}$	$x_{MgO, wf}$	$x_{SiO2, wf}$	$x_{Al2O3, wf}$	$x_{others, wf}$	$x_{CO2, wf}$ [1]
				wt%		
Limestone	55.1	0.7	0.4	0.1	0.2	43.5

Table 2. Composition of wood pellets; H_u—net calorific value, γ_i—fuel mass fraction of component i, ar: as received, wf: water free, waf: water and ash free, FC: fixed C, V: volatiles.

	$H_{u,ar}$	$\gamma_{H2O,ar}$	$\gamma_{ash,wf}$	$\gamma_{V,waf}$	$\gamma_{FC,waf}$	$\gamma_{C,waf}$	$\gamma_{H,waf}$	$\gamma_{N,waf}$	$\gamma_{S,waf}$	$\gamma_{Cl,waf}$
	kJ/kg					wt%				
Wood pellets	17,358	6.0	0.2	82.7	17.3	50.8	6.1	0.2	0.1	0.02

3. Results and Discussion

Experiments were conducted with a combustion temperature of 919 ± 8 °C and a constant limestone make-up of 0.17 mol CaO per mol C in the biomass that is fed into the gasifier. Impacts of the gasification temperature, S/C ratio and WHSV on the composition of the syngas considering permanent gases, lower hydrocarbons and tars were evaluated amongst others.

3.1. Permanent Gases and Lower Hydrocarbons

This chapter focuses on the influence of gasification temperature, S/C ratio and WHSV on the gas volume fractions of the permanent gases (H_2, CO, CO_2 and CH_4) and lower hydrocarbons (C_2H_4, C_2H_6, C_3H_6, C_3H_8 and C_4H_{10}) in the syngas. Besides a suitable composition in terms of H_2/CO/CO_2 ratio, special attention needs to be paid to the contents of CH_4 and lower hydrocarbons (C_xH_y) in the syngas. In most of the synthesis processes, CH_4 and C_xH_y are inert and not wanted as they cannot be converted. Therefore, those components need to be converted and/or removed from the syngas prior to the synthesis process, which causes additional efforts for the syngas conditioning.
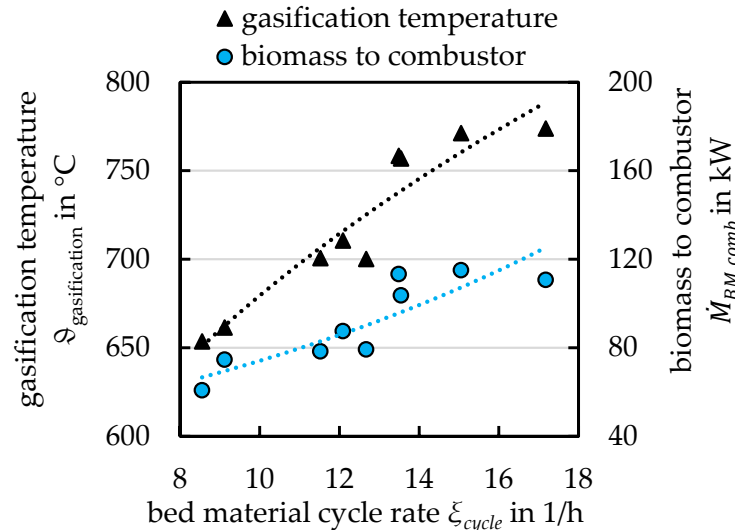
3.1.1. Influence of the Gasification Temperature

To demonstrate the influence of the gasification temperature on the permanent gases, experiments with gasification temperatures between 654 and 774 °C were conducted and compared to each other. Operational parameters such as S/C ratio (1.52 ± 0.02 mol/mol), WHSV (0.73 ± 0.03 1/h) and the biomass feed into the gasifier (30 kg/h, 138 kW) were kept constant. The gasification temperature was increased from 654–774 °C by adjusting the bed material cycle rate ξ_{cycle} (Equation (4)), as can be seen in Figure 5. The bed material cycle rate in this case expresses the solid mass flow into the gasifier related to the gasifier bed mass. Due to the enhanced bed material cycle rate that is necessary to compensate for the increasing energy demand at higher gasification temperatures, more additional biomass is required in the combustor [27]. Therefore, the feed of biomass into the combustor had to be increased from 61 kW to 115 kW within the investigated temperature range (Figure 5). The high amount of additional biomass is mainly necessary as the heat losses of the facility are rather high. In commercial scale facilities with a better surface to volume ratio, heat losses would be lower and much less additional biomass would be needed. According to calculations of Brellochs for SEG in commercial scale, at gasification temperatures < 685 °C almost no additional fuel would be needed [27,28].

Bed material cycle rate

$$\xi_{cycle} = \frac{\dot{M}_{bed,comb.\rightarrow gasifier}}{M_{bed,gasifier}} \quad \left[\frac{1}{h}\right] \tag{4}$$

(ξ_{cycle}—bed material cycle rate, $\dot{M}_{bed,comb.\rightarrow gasifier}$—mass flow of bed material from the combustor to the gasifier, $M_{bed,gasifier}$—mass of bed material within the gasifier)


Figure 5. Correlation between bed material cycle rate and gasification temperature as well as biomass mass flow into the combustor, respectively.

The influence of the gasification temperature on the composition of the permanent gases is presented in Figure 6, in which the gas volume fractions (dry basis (db) and N_2-free) of H_2, CO, CO_2 and CH_4 are plotted against the gasification temperature. Increasing the gasification temperature results in a lower hydrogen content, which is decreasing from 77 to 55 vol% within the investigated temperature range. Such high H_2 concentrations are a result of the shift of the water–gas shift reaction (Equation (3)) towards the product side caused by the CO_2 capture of the bed material. As less CO_2 is captured at higher temperatures, the H_2 concentration decreases. For the same reason, CO and CO_2 concentrations are increasing with increasing gasification temperature. CH_4 concentrations are decreasing from 12 to

9 vol.% (db, N_2-free) for increasing the gasification temperature from 654 to 774 °C. Similar trends have also been reported in literature [7,29].
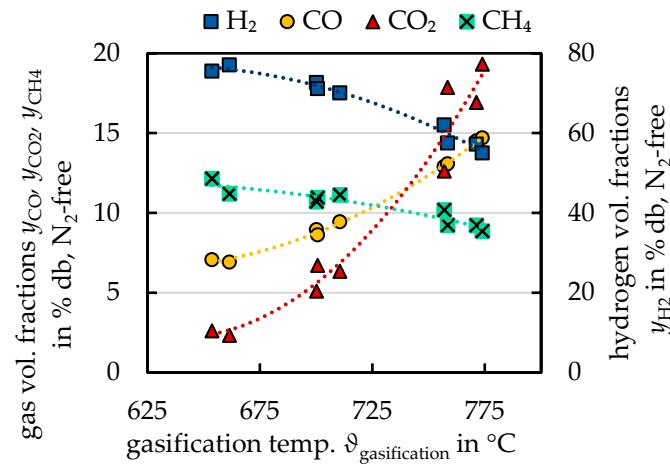
Figure 6. Gas volume fractions (db, N_2-free) of H_2, CO, CO_2 and CH_4 as a function of gasification temperature for experiments with $\varphi_{SC} = 1.52 \pm 0.02$ mol/mol and $\xi_{WHSV} = 0.73 \pm 0.03$ 1/h.

To avoid additional costs by conditioning of the syngas, the production of a syngas that is tailored for the following synthesis process is of high importance. The module M expresses the suitability of a syngas for dedicated downstream synthesis processes and is calculated according to Equation (1). For the investigated gasification temperatures, modules M between 8 and 1 were achieved as can be seen in Figure 7, showing a high flexibility of the process. By adjusting the gasification temperature, the syngas can be tailored e.g., to produce H_2 (M as high as possible), Bio-SNG (M = 3) or MeOH/DME (M = 2).
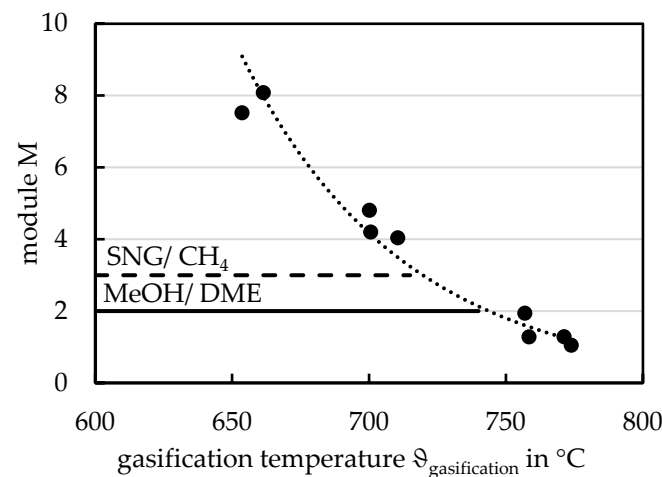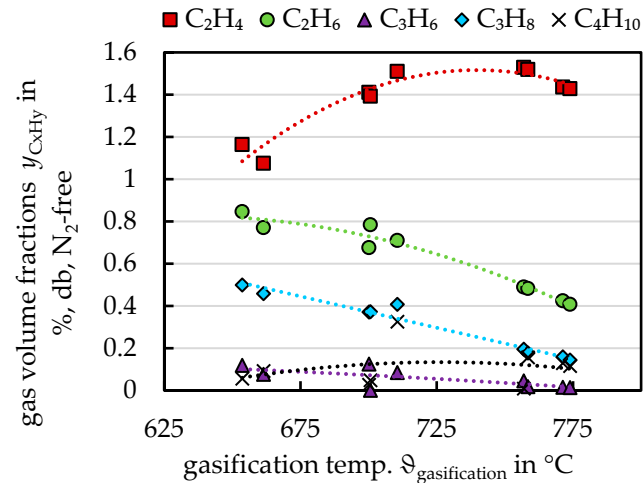

Figure 7. Module M as a function of gasification temperature for experiments with $\varphi_{SC} = 1.52 \pm 0.02$ mol/mol and $\xi_{WHSV} = 0.73 \pm 0.03$ 1/h.

Gas volume fractions of C_2H_4, C_2H_6, C_3H_6, C_3H_8 and C_4H_{10} are shown in Figure 8. The gas volume fraction of C_2H_4 increases with increasing gasification temperature up to a temperature of about 760 °C. At higher temperatures it decreases slightly. The gas volume fractions of C_2H_6, C_3H_6 and C_3H_8 are decreasing with increasing temperature, while for C_4H_{10} no clear trend can be noticed. Such trends for C_2H_4 and C_2H_6 have also been observed by Schmid et al. [29].

Sorption enhanced gasification under the above-mentioned conditions led to syngas yields between 0.6 and 1 m^3/kg (STP, N_2-free gas and waf biomass). According to Herguido et al. [30], the increase of the gas yield with the temperature is due to a higher

gas production during pyrolysis and the endothermic char gasification reactions. It is further increased by enhanced steam cracking and reforming of tars. Due to the therefore enhanced biomass conversion at higher temperatures, the gas yield increases with increasing gasification temperature.

Figure 8. Gas volume fractions (db, N_2-free) of C_2H_4, C_2H_6, C_3H_6, C_3H_8 and C_4H_{10} as a function of gasification temperature for experiments with $\varphi_{SC} = 1.52 \pm 0.02$ mol/mol and $\xi_{WHSV} = 0.73 \pm 0.03$ 1/h.

3.1.2. Influence of the Steam to Carbon Ratio

Investigations regarding the influence of the steam to carbon ratio on the composition of the permanent gases were conducted at a constant gasification temperature of 658 ± 8 °C and a WSHV of 0.74 ± 0.04 1/h. The S/C ratio (calculated according to Equation (5)) was varied by adjustment of the steam mass flow into the gasifier while keeping the biomass feed constant. The mass flow of the biomass was equal to the temperature variation experiments. By changing the S/C ratio via steam mass flow it can be ensured that the WHSV remains more or less the same in all experiments, which would not be the case if the biomass mass flow would be adjusted. Reduction of the gasification temperature due to higher steam mass flows was compensated for by modification of the bed material cycle rate.
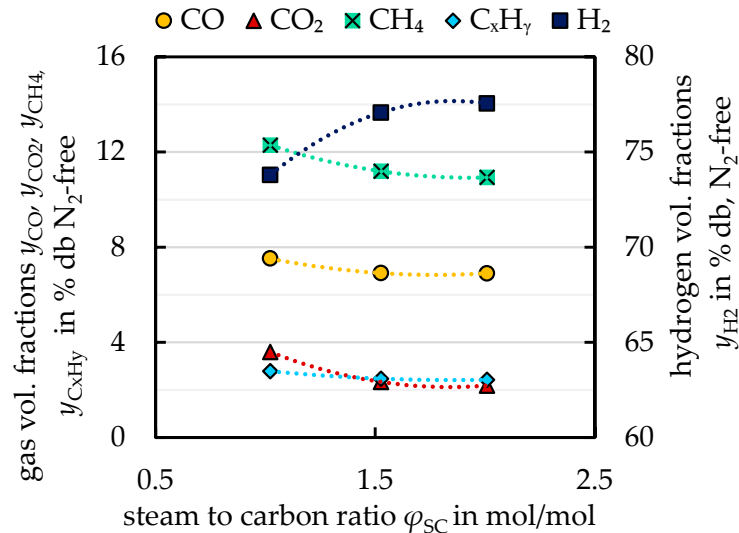
Steam to carbon ratio:

$$\varphi_{SC} = \frac{\dot{N}_{H_2O,gasifier}}{\dot{N}_{C,fuel,gasifier}} = \frac{\dot{N}_{steam,gasifier} + \dot{N}_{H_2O,fuel,gasifier}}{\dot{N}_{C,fuel,gasifier}} \left[\frac{mol}{mol}\right] \qquad (5)$$

(φ_{SC}—steam to carbon ratio, $\dot{N}_{H_2O,gasifier}$—molar flow rate of H_2O fed into the gasifier, $\dot{N}_{C,fuel,gasifier}$—molar flow rate of fuel carbon fed into the gasifier, $\dot{N}_{steam,gasifier}$—molar flow rate of steam fed into the gasifier, $\dot{N}_{H_2O,fuel,gasifier}$—molar flow rate of fuel moisture fed into the gasifier)

Figure 9 shows moisture and N_2-free gas volume fractions of H_2, CO, CO_2, CH_4 and C_xH_y for S/C ratios between 1 and 2 mol/mol. By enhancing the steam content in the gasifier, higher hydrogen and lower CO gas volume fractions can be reached. This behavior leads to the assumption that the WGS reaction is shifted towards the product side as the backwards reaction is inhibited by the enhanced partial pressure of steam inside the reactor, which has also been observed by [19,29]. The CO_2 gas volume fraction on the other hand is decreasing with increasing S/C ratio as is the CO_2 gas yield, which might be due to the higher bed material cycle rate at higher S/C ratios, resulting in a higher amount of fresh CaO inside the gasifier and causing a higher CO_2 capture. This can be confirmed by the change of the mass flow of $CaCO_3$ that is transferred from the gasifier into the combustor, which is increasing with increasing S/C ratio, showing that more CO_2 is captured. The

lower CO_2 partial pressure also contributes to the increased shift of the WGS reaction. Increasing the S/C ratio seems also to be beneficial for reducing the content of CH_4 and C_xH_y components in the syngas, which is in line with literature data [19,29].

Figure 9. Gas volume fractions (db, N_2-free) as a function of steam to carbon ratio for experiments with $\vartheta_{gasification} = 658 \pm 8\ ^\circ C$ and $\xi_{WHSV} = 0.70 \pm 0.03$ 1/h.

As has been shown, increasing the S/C ratio leads to better syngas qualities in terms of higher hydrogen and lower CH_4 and C_xH_y contents. However, we must take into account the fact that a higher steam mass flow also results in a higher energy demand [31] and also the amount of wastewater that needs to be disposed increases. Therefore, it needs to be considered carefully whether the advantages or disadvantages of higher S/C ratios are predominating.

### 3.1.3. Influence of the Weight Hourly Space Velocity

For investigating the influence of the weight hourly space velocity (WHSV) on the composition of the syngas, experiments with two different WHSVs (0.68 and 0.85 1/h) were carried out. The WHSV was modified by changing the amount of bed material inside the gasifier with about 48 kg for WHSV = 0.68 1/h and about 38 kg for 0.85 1/h. The amount of bed material was calculated based on pressure differences inside the reactor. The WHSV is calculated according to Equation (6). The mass flow of biomass was kept constant between the experiments with a fuel input of 138 kW. The mass fraction of CaO inside the reactor bed was determined based on the analysis of solid samples taken from the bottom loop seal of the gasifier. Gasification temperature and S/C ratio were adjusted to $651 \pm 1\ ^\circ C$ and 1.52 ± 0.02 mol/mol, respectively.

Weight hourly space velocity:

$$\xi_{WHSV} = \frac{\dot{M}_{biomass,waf,gasifier}}{x_{CaO,bed,gasifier} \cdot M_{bed,gasifier}} \quad \left[\frac{1}{h}\right] \tag{6}$$

(ξ_{WHSV}—weight hourly space velocity, $\dot{M}_{biomass,waf,gasifier}$—mass flow of water and ash free biomass fed into the gasifier, $x_{CaO,bed,gasifier}$—mass fraction of CaO within the gasifier bed, $M_{bed,gasifier}$—mass of bed material within the gasifier).

Figure 10 presents the gas volume fractions (dry, N_2-free) of the different permanent gas species and C_xH_y for two different WHSVs. The H_2 concentration decreases from 79 to 77 vol% for increasing WHSV, while the CO concentration increases (6.0 to 7.1 vol.%). This could be explained by a more pronounced WGS reaction in the case of the lower WHSV due to a higher bed mass resulting in longer residence times of the gas molecules inside the bed. As the CO_2 concentration remains about constant when changing the WHSV, it is assumed that the CO_2 capture in this case is limited by the thermodynamic equilibrium. Otherwise one would expect higher CO_2 concentrations for an enhanced WHSV due to lower residence times inside the bed as was observed in semi-batch experiments by Poboss and Corella et.al. [19,32]. Both CH_4 and C_xH_y concentrations are enhanced for a WHSV of 0.85 1/h compared to 0.68 1/h, which is most likely due to the lower residence time in the case of WHSV = 0.85 1/h. For the same reason, according to Poboss' [20] semi-batch experiments, also the tar yield is increased for higher WHSVs. As tars have not been measured at both WHSVs, this result cannot be proved in this study.
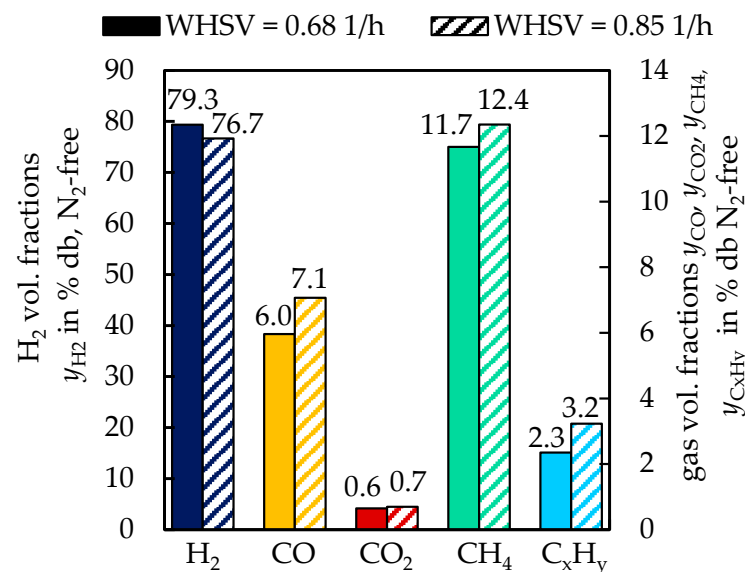
Figure 10. Gas volume fractions (db, N_2-free) for ξ_{WHSV} = 0.68 and 0.85 1/h for experiments with $\vartheta_{gasification}$ = 651 ± 1 °C and φ_{SC} = 1.52 ± 0.02 mol/mol.

According to those results, a WHSV of 0.68 1/h seems to be more beneficial in terms of high H_2 and low CH_4 and C_xH_y gas volume fractions in the syngas compared to a WHSV of 0.85 1/h under the described operational conditions. That trend is in line with the observations of several authors in the literature [19,32].

3.2. Tars

Reformation of tars is one of the main challenges in fluidized bed gasification [33] of biomass. To avoid problems such as clogging caused by condensation of tars or pollution of wastewater streams by water soluble tars, tar formation should be prevented or reduced if possible. As knowledge of tar formation is essential for the design of new plants and syngas cleaning, the influence of gasification temperature and S/C ratio on the tar

content in the syngas was investigated under the operational conditions that are described in Sections 3.1.1 and 3.1.2 respectively. Gravimetric and GC-FID tar concentrations were analyzed as described in Section 2.1.

3.2.1. Influence of the Gasification Temperature

Gravimetric and GC-FID tar concentrations (on db, at standard temperature and pressure (STP)) are plotted in Figure 11 for gasification temperatures between 654 and 771 °C. The trends indicate a significant influence of the gasification temperature on the tar concentration with enhanced tar reforming for increasing gasification temperature as it is also reported in [19,29,34,35]. By increasing the gasification temperature from 654–771 °C, the gravimetric tar content is reduced significantly from 23–1 g/m^3 (db, STP) while the GC-FID tars decrease from 18–4 g/m^3 (db, STP). For gasification temperatures > 660 °C, the syngas comprises a higher amount of GC-FID tars than gravimetric tars. This indicates that the share of lighter tar components is enhanced at such high temperatures. The tar species considered in the GC-FID analysis (see Section 2.1) were classified according to standards of the Energy research Center of the Netherlands (ECN) as described in [36]. Class 1 tars represent gravimetric tar species [10] which are not detectable by GC-FID analysis and could therefore not be quantified. During SEG with wood pellets the tar classes 2–5 show a decreasing trend with increasing gasification temperature. At gasification temperatures up to about 715 °C, GC-FID tars mainly consist out of class 2 (heterocyclic aromatic compounds [36]) and class 3 (aromatic compounds [36]) tars, while at higher temperatures class 3 and class 4 (2–3 ring polyaromatic hydrocarbons [36]) tars are the major components as can be seen in Figure 12. The quantity of class 5 (4–7 ring polyaromatic hydrocarbons [36]) tars is for the whole temperature range the lowest.
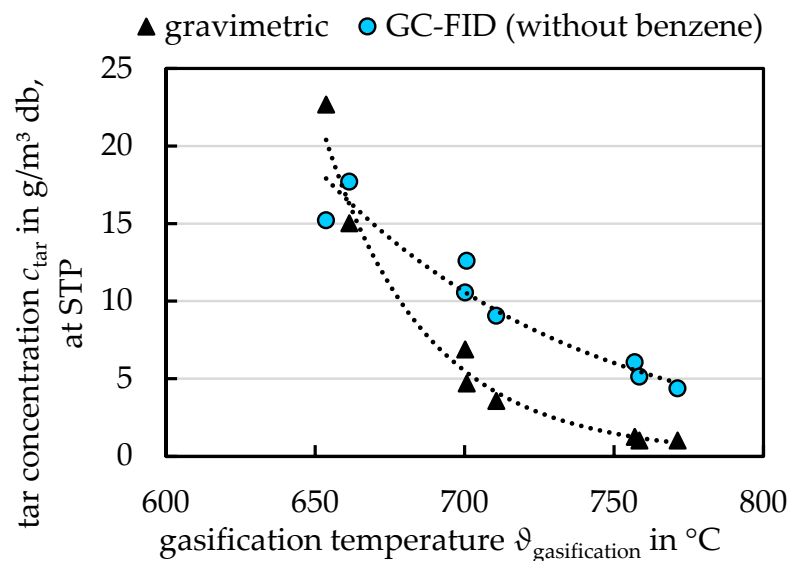

Figure 11. Gravimetric and gas chromatography and flame ionization detector (GC-FID) tar concentrations as a function of gasification temperature for experiments with $\varphi_{SC} = 1.52 \pm 0.02$ mol/mol and $\xi_{WHSV} = 0.73 \pm 0.03$ 1/h.
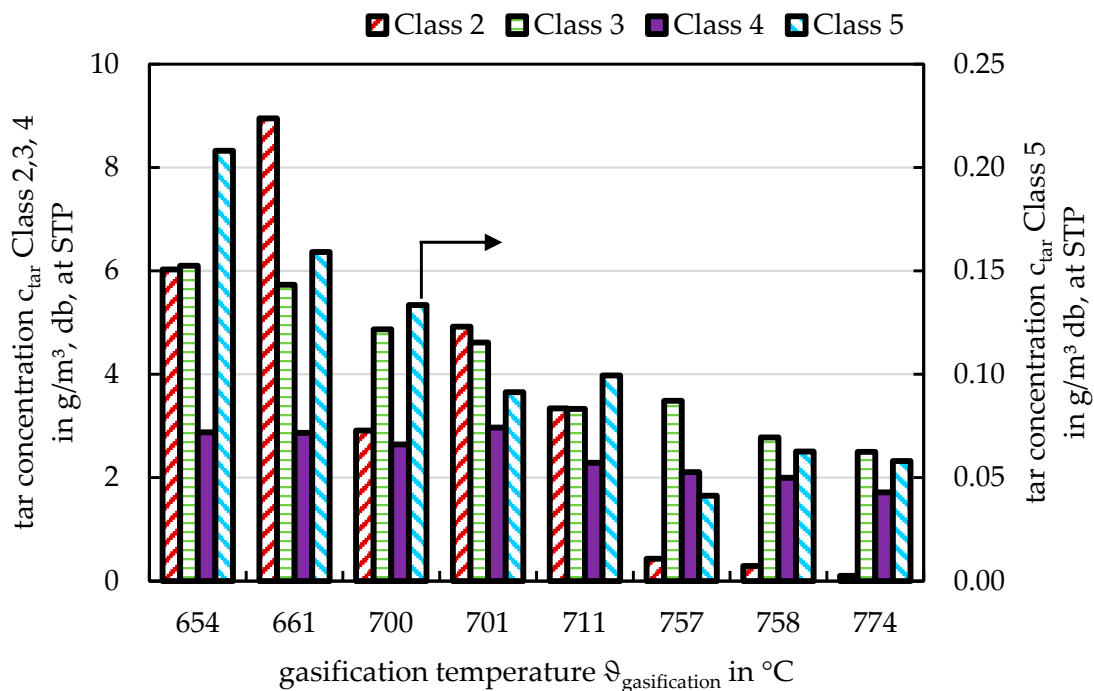
Figure 12. GC-FID tar concentrations for class 2, 3, 4 and 5 tars as a function of gasification temperature for experiments with φ_{SC} = 1.52 $\pm$ 0.02 mol/mol and ξ_{WHSV} = 0.73 $\pm$ 0.03 1/h.

3.2.2. Influence of the Steam to Carbon Ratio

Figure 13 illustrates the gravimetric tar content (db, N_2-free, STP) for S/C ratios between 1 and 2 mol/mol at a gasification temperature of 658 $\pm$ 8 °C. The gravimetric tar concentration is significantly reduced from 21 to 9 g/m^3 (db, N_2-free, STP) when enhancing the S/C ratio from 1–2 mol/mol, showing a strong influence of the S/C ratio on the tar reforming as has also been noted in literature [19,30,37].
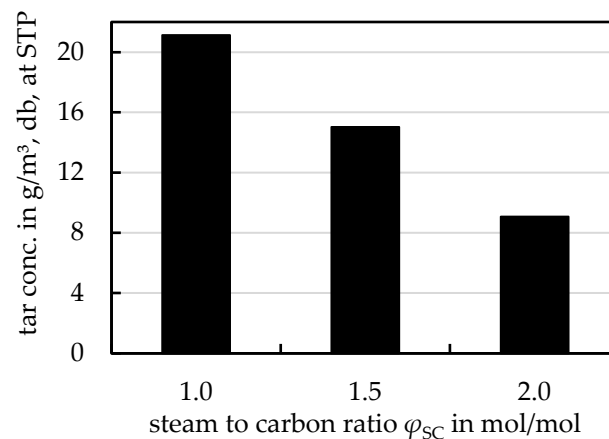
Figure 13. Gravimetric tar concentration as a function of steam to carbon ratio for experiments with $\vartheta_{gasification}$ = 658 $\pm$ 8 °C and ξ_{WHSV} = 0.70 $\pm$ 0.03 1/h.

However, it also needs to be noted that due to the higher bed material cycle rate at higher S/C ratios that is necessary to maintain a constant gasification temperature (as described in Section 3.1.2), the mass flow of CaO entering the gasifier also increases, promoting the tar reforming due to the catalytic effect of CaO [8]. Hence the results reveal the overlapping effects of an increased S/C ratio and a higher mass flow of CaO into the gasifier.

4. Conclusions

Investigations on the influence of gasification temperature, steam to carbon ratio and weight hourly space velocity on the syngas composition in the SEG process were carried out in a 200 kW DFB pilot scale facility using wood pellets as biomass and limestone as CO_2-active bed material. The results obtained show a strong dependence of the syngas composition on the gasification temperature with high gasification temperatures being beneficial in terms of high gas yield and low tar content, but disadvantageous regarding a high share of hydrogen in the syngas. Increasing the gasification temperature led to higher gas volume fractions of C_2H_4 while the share of all other C_xH_y components diminished. The gravimetric and GC-FID tar contents could be reduced to 1 and 4 g/m^3 (db, STP), respectively, by increasing the gasification temperature up to 771 °C. Moreover, investigations of the S/C ratio at a gasification temperature of 658 ± 8 °C revealed increased hydrogen and reduced CO, CO_2, CH_4 and C_xH_y gas volume fractions in the syngas for increasing the S/C ratio from 1–2 mol/mol. The S/C ratio also strongly influenced the amount of tars in the syngas. Increasing the S/C ratio resulted in a reduction of the gravimetric tars from 21 to 9 g/m^3 (db, STP). Those results indicate an enhanced WGS reaction and a better reformation of CH_4, C_xH_y hydrocarbons and tars due to the higher steam content inside the reactor. Experiments focusing on the impact of the WHSV indicated that a lower WHSV seems to be more beneficial in terms of high H_2 and low CH_4 and C_xH_y gas volume fractions.

Overall, it has been shown that the syngas composition can be adjusted by several parameters to be suitable for different downstream synthesis processes, with the gasification temperature being the most influential parameter. This makes SEG to a very promising process for the production of tailored synthesis gases.

Abbreviations

ar	as received
BFB	bubbling fluidized bed
BM	biomass
CCS	carbon capture and storage
CFB	circulating fluidized bed
DFB	dual fluidized bed
DME	dimethyl ether
ECN	Energy research Center of the Netherlands
FC	fixed carbon
FT	Fischer–Tropsch
GC-FID	gas chromatography and flame ionization detector
GHG	greenhouse gas

MeOH	methanol
NDIR	nondispersive infrared sensor
S/C	steam to carbon
SEG	sorption enhanced gasification
SNG	synthetic natural gas
STP	standard temperature and pressure (0 °C and 1013 mbar)
V	volatiles
waf	water and ash free
wf	water free
WGS	water-gas-shift
WHSV	weight hourly space velocity

Symbols

c_{tar}	g/m^3	tar mass in dry and N$_2$-free gas at STP
H_u	kJ/kg	net calorific value
$\dot{M}$	kg/s	mass flow
M	kg	mass
$\dot{N}$	mol/s	mole flow
p	Pa	pressure
x_i	wt.%	mass fraction of component i
y_i	vol.%	gas volume fraction of component i
γ_i	wt.%	fuel mass fraction of component i
ΔH_R	kJ/mol	specific reaction enthalpy
ϑ	°C	temperature
ξ_{CaO}	1/h	bed material cycle rate
ξ_{WHSV}	1/h	weight hourly space velocity
φ_{SC}	mol/mol	steam to carbon ratio

References

1. European Commission. 2030 Climate & Energy Framework. Available online: https://ec.europa.eu/clima/policies/strategies/2030_en (accessed on 17 December 2020).
2. Ellen MacArthur Foundation. *Growth within: A Circular Economy Vision for a Competitive Europe*; McKinsey & Company: New York, NY, USA, 2015.
3. Iaquaniello, G.; Centi, G.; Salladini, A.; Palo, E.; Perathoner, S. Waste to Chemicals for a Circular Economy. *Chem. Eur. J.* **2018**, *24*, 11831–11839. [CrossRef] [PubMed]
4. Rauch, R.; Hrbek, J.; Hofbauer, H. Biomass gasification for synthesis gas production and applications of the syngas. *WIREs Energy Environ.* **2014**, *3*, 343–362. [CrossRef]
5. Benedikt, F.; Fuchs, J.; Schmid, J.C.; Müller, S.; Hofbauer, H. Advanced dual fluidized bed steam gasification of wood and lignite with calcite as bed material. *Korean J. Chem. Eng.* **2017**, *34*, 2548–2558. [CrossRef]
6. Corella, J.; Toledo, J.M.; Molina, G. A Review on Dual Fluidized-Bed Biomass Gasifiers. *Ind. Eng. Chem. Res.* **2007**, *46*, 6831–6839. [CrossRef]
7. Fuchs, J.; Schmid, J.C.; Müller, S.; Hofbauer, H. Dual fluidized bed gasification of biomass with selective carbon dioxide removal and limestone as bed material: A review. *Renew. Sustain. Energy Rev.* **2019**, *107*, 212–231. [CrossRef]
8. Koppatz, S.; Pfeifer, C.; Rauch, R.; Hofbauer, H.; Marquard-Moellenstedt, T.; Specht, M. H2 rich product gas by steam gasification of biomass with in situ CO2 absorption in a dual fluidized bed system of 8 MW fuel input. *FUEL Process. Technol.* **2009**, *90*, 914–921. [CrossRef]
9. Aghaalikhani, A.; Schmid, J.C.; Borello, D.; Fuchs, J.; Benedikt, F.; Hofbauer, H.; Rispoli, F.; Henriksen, U.B.; Sárossy, Z.; Cedola, L. Detailed modelling of biomass steam gasification in a dual fluidized bed gasifier with temperature variation. *Renew. Energy* **2019**, *143*, 703–718. [CrossRef]
10. Koppatz, S.; Pfeifer, C.; Hofbauer, H. Comparison of the performance behaviour of silica sand and olivine in a dual fluidised bed reactor system for steam gasification of biomass at pilot plant scale. *Chem. Eng. J.* **2011**, *175*, 468–483. [CrossRef]
11. Hofbauer, H.; Rauch, R.; Klaus, B.; Reinhard, K.; Aichernig, C. Biomass CHP Plant Güssing—A Success Story. In *Expert Meeting on Pyrolysis and Gasification of Biomass and Waste*; Bridgewater, A.V., Ed.; CPL Press: Strasbourg, France; Newbury, UK, 2002; pp. 527–536.

12. Thunman, H.; Seemann, M.; Berdugo Vilches, T.; Maric, J.; Pallares, D.; Ström, H.; Berndes, G.; Knutsson, P.; Larsson, A.; Breitholtz, C.; et al. Advanced biofuel production via gasification—lessons learned from 200 man-years of research activity with Chalmers' research gasifier and the GoBiGas demonstration plant. *Energy Sci. Eng.* **2018**, *6*, 6–34. [CrossRef]

13. Wilk, V.; Hofbauer, H. Analysis of optimization potential in commercial biomass gasification plants using process simulation. *FUEL Process. Technol.* **2016**, *141*, 138–147. [CrossRef]

14. Wilcox, J. *Carbon Capture*; Springer: Boston, MA, USA, 2012.

15. Kaltschmitt, M.; Hartmann, H.; Hofbauer, H. *Energie aus Biomasse: Grundlagen, Techniken und Verfahren*, 2nd ed.; Springer: Berlin/Heidelberg, Germany, 2009.

16. Pfeifer, C.; Puchner, B.; Hofbauer, H. In-situ CO2-absorption in a dual fluidized bed biomass steam gasifier to produce a hydrogen rich syngas. *Int. J. Chem. React. Eng.* **2007**, *5*. [CrossRef]

17. Martínez, I.; Kulakova, V.; Grasa, G.; Murillo, R. Experimental investigation on sorption enhanced gasification (SEG) of biomass in a fluidized bed reactor for producing a tailored syngas. *FUEL* **2020**, *259*, 116252. [CrossRef]

18. Pitkäoja, A.; Ritvanen, J.; Hafner, S.; Hyppänen, T.; Scheffknecht, G. Simulation of a sorbent enhanced gasification pilot reactor and validation of reactor model. *Energy Convers. Manag.* **2020**, *204*, 112318. [CrossRef]

19. Poboß, N. *Experimentelle Untersuchung der sorptionsunterstützten Reformierung*; Universität Stuttgart: Stuttgart, Germany, 2016.

20. Valverde, J.M.; Sanchez-Jimenez, P.E.; Perez-Maqueda, L.A. Limestone Calcination Nearby Equilibrium: Kinetics, CaO Crystal Structure, Sintering and Reactivity. *J. Phys. Chem. C* **2015**, *119*, 1623–1641. [CrossRef]

21. Schweitzer, D.; Beirow, M.; Gredinger, A.; Armbrust, N.; Waizmann, G.; Dieter, H.; Scheffknecht, G. Pilot-Scale Demonstration of Oxy-SER steam Gasification: Production of Syngas with Pre-Combustion CO_2 Capture. *Energy Procedia* **2016**, *86*, 56–68. [CrossRef]

22. Dieter, H. Gasification with In-Situ CO_2 Capture and Separation in a 200 kWth Pilot Plant. In Proceedings of the Gasification Technologies Conference, Washington, DC, USA, 26–29 October 2014.

23. Schmid, M.; Beirow, M.; Schweitzer, D.; Waizmann, G.; Spörl, R.; Scheffknecht, G. Product gas composition for steam-oxygen fluidized bed gasification of dried sewage sludge, straw pellets and wood pellets and the influence of limestone as bed material. *Biomass Bioenergy* **2018**, *117*, 71–77. [CrossRef]

24. Kübel, M.; Gfrereis, C.; Waizmann, J.; Michel, M.; Hein, K.R. Hydrogen Rich Syngas Production from Steam Gasification of BCO in a FB Reactor-Gas Composition and Tar Formation at Various Conditions. In Proceedings of the 2nd World Biomass Conference-Biomass for Energy, Industry and Climate Protection, Rome, Italy, 10–14 May 2004; pp. 763–766.

25. CEN/TC BT/TF 143. *Biomass Gasification—Tar and Particles in Product Gases—Sampling and Analysis*; 2004.

26. Van Paasen, S.V.B.; Kiel, J.H.A. Tar Formation in Fluidised-Bed Gasification—Impact of Gasifier Operating Conditions. In Proceedings of the 2nd World Conference and Technology Exhibition on Biomass for Energy, Industry and Climate Protection, Rome, Italy, 10–14 May 2004.

27. Brellochs, J. Experimentelle Untersuchung und Prozess-Simulation der AER-Biomassevergasung zur Erzeugung eines regenerativen Erdgassubstitutes. Ph.D. Thesis, Universität Stuttgart, Stuttgart, Germany, 2014.

28. Schweitzer, D.; Albrecht, F.; Schmid, M.; Beirow, M.; Spörl, R.; Dietrich, R.; Seitz, A. Process Simulation and Techno-Economic Assessment of SER Steam Gasification for Hydrogen Production. *Int. J. Hydrogen Energy* **2018**, *3*, 569–579. [CrossRef]

29. Schmid, J.; Fuchs, J.; Benedikt, F.; Mauerhofer, A.; Müller, S.; Hofbauer, H.; Stocker, H.; Kieberger, N.; Bürgler, T. Sorption Enhanced Reforming with the Novel Dual Fluidized Bed Test Plant at TU Wien. In Proceedings of the 25th European Biomass Conference and Exhibition, Stockholm, Sweden, 12–15 June 2017.

30. Herguido, J.; Corella, J.; Gonzalez-Saiz, J. Steam Gasification of Lignocellulosic Residues in a Fluidized Bed at a Small Pilot Scale. Effect of the Type of Feedstock. *Ind. Eng. Chem. Res.* **1992**, *31*, 1274–1282. [CrossRef]

31. Weimer, T.; Berger, R.; Hawthorne, C.; Abanades, J.C. Lime enhanced gasification of solid fuels: Examination of a process for simultaneous hydrogen production and CO2 capture. *FUEL* **2008**, *87*, 1678–1686. [CrossRef]

32. Corella, J.; Toledo, J.M.; Molina, G. Steam Gasification of Coal at Low$-$Medium (600$-$800 °C) Temperature with Simultaneous CO_2 Capture in a Bubbling Fluidized Bed at Atmospheric Pressure. 2. Results and Recommendations for Scaling Up. *Ind. Eng. Chem. Res.* **2008**, *47*, 1798–1811. [CrossRef]

33. Göransson, K.; Söderlind, U.; He, J.; Zhang, W. Review of syngas production via biomass DFBGs. *Renew. Sustain. Energy Rev.* **2011**, *15*, 482–492. [CrossRef]

34. Corella, J.; Toledo, J.M.; Molina, G. Biomass gasification with pure steam in fluidised bed: 12 variables that affect the effectiveness of the biomass gasifier. *Int. J. Oil Gas. Coal Technol.* **2008**, *1*, 194–207. [CrossRef]

35. Schmid, J.C.; Benedikt, F.; Fuchs, J.; Mauerhofer, A.M.; Müller, S.; Hofbauer, H. Syngas for biorefineries from thermochemical gasification of lignocellulosic fuels and residues—5 years' experience with an advanced dual fluidized bed gasifier design. *Biomass Conv. Bioref.* **2019**. [CrossRef]

36. Kiel, J.; van Paasen, S.; Neeft, J.; Devi, L.; Ptasinski, K.; Janssen, F.J.J.G. *Primary Measures to Reduce Tar Formation in Fluidised-Bed Biomass Gasifiers*; Final report SDE project P1999-012; ECN: Petten, The Netherlands, 2004.

37. Udomsirichakorn, J.; Basu, P.; Salam, P.A.; Acharya, B. Effect of CaO on tar reforming to hydrogen-enriched gas with in-process CO_2 capture in a bubbling fluidized bed biomass steam gasifier. *Int. J. Hydrogen Energy* **2013**, *38*, 14495–14504. [CrossRef]